A FCG MODEL AND THE GRAPHICAL USER INTERFACE UNDER MATLAB FOR PREDICTING FATIGUE LIFE: PARAMETRIC STUDIES

Tayeb Kebir [a,*]   0000-0002-1843-6529
José A.F.O. Correia [b]   0000-0002-4148-9426
Mohamed Benguediab [c]   0000-0003-1523-2798
Abdellatif Imad [d]   0000-0002-3174-987X

[a] Department of Technical Sciences, Institute of Science and Technology,
University Center Salhi Ahmed, Naama, Algeria.
[b] Researcher & Invited Professor, CONSTRUCT & Faculty of Engineering,
University of Porto, 4200-465 Porto, Portugal.
[c] Laboratory of Materials and Systems Reactive, Faculty of Technology,
Universty of Sidi Bel Abbes, Algeria.
[d] Laboratory of Mechanical of Lille, University of Lille1, Polythech'Llle1, France.

*kebir.tayeb@cuniv-naama.dz

Abstract

The focus of this research work was predicting the fatigue life of mechanical components used for industrial and transport systems. To understand how the phenomenon of fatigue occurs in a material, the fatigue crack growth is studied. The purpose of this work was to create a graphical user interface (GUI) under Matlab to allow researchers to conduct the parametric studies of fatigue crack propagation to predict fatigue life. In this work, three models for fatigue crack propagation were used: those of Paris, Walker and Forman in order to study the three parameters: the Paris exponent m, load ratio R and hardness K_{IC}, respectively. In addition, a novel model FCG was developed to study the influence of the hardening parameters (K', n') on fatigue crack propagation. The comparison of the simulation results with those in the literature shows good agreement.

Keywords: Fatigue life prediction; Graphical User Interface, fatigue crack growth; cyclic hardening; Paris; Walker; Forman
Article Category: Research Article

INTRODUCTION

Fatigue is likely to cause the destruction of structural a component over number of cycles. Fatigue begins with a local plastic deformation without plasticization of

the whole structure, occurring first around the defect and then at the end of the crack once it has formed (and propagated). The initial crack and fatigue crack growth represent a major part of the fatigue life of a material. By applying the principles of fracture mechanics, it is possible to predict the number of cycles causing a crack of a certain length to failure. The velocity of fatigue crack growth varies linearly with the stress intensity factor range (ΔK) on bi-logarithmic scale. The crack most often propagates on a plane perpendicular to the direction of the load applied. This regime is characterized by the gradual acceleration of the crack propagation when the stress intensity factor (ΔK) increases. (Paris-Erdogan 1963) linked the velocity of fatigue crack propagation with the amplitude of the stress intensity factor (ΔK) by a power type relation known as the Paris law (Table 1). Furthermore, there are several models predicting the fatigue crack propagation which express the fatigue life along the crack length; these models are initially based on one of the three approaches presented to quantify the damage at the crack tip. Moreover, the models based on the accumulation of the damage are the least used since it is difficult to quantify the damage necessary for the crack propagation [1], [2]. Models excluding closure are frequently used in the literature because of their simplicity and their good comparison with experimental results. The FCG models developed by different authors can be classified according to their materials parameters and role as presented in Table 1. Fatigue resistance of a material depends on number of parameters such as the material's chemical composition, mechanical properties, heat treatment conditions, loads and the environment. The explanation of this phenomenon has been the subject of several works for different materials taking into account the influence of several intrinsic and extrinsic factors such as the load ratio [3], [4], geometry of specimen [3], thickness [5], cyclic plastic hardening [2], cyclic plastic deformation [6], [7], ageing of materials [8], temperature [9]. The influence of the variability of these parameters on the velocity of fatigue crack propagation and fatigue life prediction were studied by several authors [2], [6], [10], [11].

Table 1. Different models for FCG with their materials parameters.

	Materials	C [m/cycle]	m	ΔK_{th} [MPa.m$^{1/2}$]	R	Refs
Paris model $$\frac{da}{dN} = C(\Delta K)^m$$	S355NL	2.10E-13	4.23	6.57	0.1	[12]
		8.10E-14	4.62	6.43	0.3	
		2.10E-13	4.16	5.42	0.5	
	316L	0.40 E-13	5.39	3.20	0	[13]
		0.40E-13	5.71	2.85	0.12	
		1.60E-13	5.73	2.25	0.217	
		2.19 E-13	5.77	2.10	0.334	
		3.88 E-13	5.70	2.02	0.44	
	304L	1.987E-11		2.095	0	[13]
		4.2 E-11	4.315	1.768	0.176	
		4.33 E-11		1.749	0.264	
		4.79 E-11		1.709	0.334	

Material	C	m	ΔK_th	R	Ref
	5.03 E-11		1.690	0.39	
	5.63 E-11		1.646	0.44	
	5.583E-12	2.7	9.5	0	[14]
	1.796E-11	2.7	8.6	0	
	1.359E-11	2.8	8.4	0	
	1.327E-11	2.8	8.35	0	
Nickel Chrome 12NC6	8.05E-8	2.00		0.05	[4], [15]
	4.02E-8	2.25		0.1	
	5.43E-9	2.97		0.3	
	2.87E-9	3.20		0.5	
2024 T3	4.9423E-11	2.6526	1.999	-1	[16]
	2.238E-10		1.146	0	
	2.6029E-10		1.0839	0.1	
7075-T6	7.2965E-10	2.3398	0.5202	0	[16]
	1.6170E-11		1.0034	-1	
	8.65E-11	3.49		0.1	[17]
	4.37E-11	3.21		0	
	1,47E-11	3.40		-0.33	
	3.89E-12	3.49		-0.60	
	9.83E-11	3.64		0.0	[18]
	4.72E-12	4.13		0.2	
	2.86E-10	3.59		0.33	
	3.40E-10	3.64		0.5	
	3.55E-11	4.14		0.67	
	3.86E-12	4.68		0.8	
6082-T6	1.2E-10	3.40		0.40	[19]
	8.9E-10	3.45		0.25	
	5.1E-10	3.54		0.50	
	1.9E-10	3.98		-0.25	
Ti-6Al-4V	7,3017E-11	2.3779	1.4687	-1	[16]
	1,6580E-10		1.0434	0.1	
	2,2273E-10		0.9215	0.5	

Walker model

$$\frac{da}{dN} = \frac{C}{\left(1 - R\right)^{m(1-\gamma)}} \left(\Delta K\right)^m$$

Material	C_0 [m/cycle]	m	ΔK_{th} [MPa.m$^{1/2}$]	γ	R	Ref
2019-T851			2.75	3.998	0.0	[20]
			2.59	3.389	0.1	
			2.25	3.494	0.3	
			1.86	3.937	0.5	
			1.40	3.590	0.7	

		C	m	ΔK_{th} [MPa.m$^{1/2}$]	K_{IC} [MPa.m$^{1/2}$]	R	
				1.12	2.429	0.8	
	2024-T3	0.158E-8	3.301		0.164	-1	[21]
		0.167E-8	3.273		0.618	0.5	
	7075-T6	2.66E-11	3.84		0.564	0.2	[18]

Forman model

$$\frac{da}{dN} = \frac{C(\Delta K)^m}{(1-R)(K_{IC}-\Delta K)}$$

and

Forman modified model

$$\frac{da}{dN} = \frac{C(\Delta K - \Delta K_{th})^m}{(1-R)(K_{IC}-\Delta K)}$$

Material	C	m	ΔK_{th} [MPa.m$^{1/2}$]	K_{IC} [MPa.m$^{1/2}$]	B [mm]	Ref
2024-T3	1.10E-3	0.71	6.2	29.4	1.6	[5]
	0.84E-3	0.96	5.3	29.2	3.2	
	1.07E-3	0.85	6.0	29.5	4.8	
	1.09E-3	0.36	6.7	21.2	9.8	
	4.05E-3	0.74	5.3	23.5	1.0	
	0.52E-3	0.76	5.6	26.3	3.0	
	0.25E-3	1.32	4.3	32.1	5.0	
	0.71E-3	1.03	6.2	32.3	12.5	

Material	C	m	ΔK_{th} [MPa.m$^{1/2}$]	K_{IC} [MPa.m$^{1/2}$]	R	Ref
7020-T7	1.0E-5	3.24		50.12	0.1	[22]
	2.0E-5	3.17				
	1.0E-5	3.16				
	1.33E-5	3.19				

Elber model

$$\frac{da}{dN} = C(U\Delta K)^m$$

Material	C	m	ΔK_{th} [MPa.m$^{1/2}$]	U	R	Ref
2019-T851			2.75	0.7037	0	[20]
			2.59	0.7577	0.1	
			2.25	0.8639	0.3	
			1.86	0.9124	0.5	
			1.40	0.8662	0.7	
AISI 316N	3.00E-9	4	6.00		0.45	[23]
S355NL	6.10E-12	3.40	4.25		0.1	[12]

Priddle model

$$\frac{da}{dN} = C\left(\frac{(\Delta K - \Delta K_{th})(1-R)}{((1-R).K_{IC}-\Delta K)}\right)^m$$

Material	C	m	ΔK_{th} [MPa.m$^{1/2}$]	K_{IC} [MPa.m$^{1/2}$]	ε impos	Ref
7475–T7351	3.587E-06	1.558	1.31	95.5	0%	[24]
	8.754E-06	1.750	1.45	92.8	3%	
	5647E-06	1.665	1.37	79.3	5%	

Wang model

$$\frac{da}{dN} = \frac{A.M^m}{1 - \left(\frac{K_{max}}{K_{IC}}\right)^n}$$

Material	A	m	n	K_{IC} [MPa.m$^{1/2}$]	R	Ref
AA 6013	6.0068E-10	2.60	6.00	48.35	-1	[25]
	2.9948E-10	2.70	6.00	57.03	0.1	
	1.8894E-10	2.66	6.00	62.45	0.3	
	1.5274E-10	2.61	6.00	61.67	0.5	
	9.3434E-10	2.52	6.42	65.00	0.7	

Dowling-Begley model

$$\frac{da}{dN} = \frac{C}{\sqrt{E}}\left(\Delta J\right)^{m/2}$$

	C	m	E [GPa]	ΔJ_{th}	R	
Low alloy steel	1.43E-11	2.75	206		0.2	[26]

Weertman model

$$\frac{da}{dN} = \frac{A}{\mu\sigma_e^2 U_c}\left(\Delta K\right)^4$$

	A	σ_e [MPa]	U_c [J/m²]	μ [MPa]	
2219-T861	4.50E-11	370	2.40E+5	2.60E+4	[27] [28]
	7.50E-10	370	1.60E+5	2.60E+4	
	2.04E-10	260	2.10E+5	2.60E+4	
Steel Nb-HSLA	9.00E-12	340	6.00E+5	7.80E+4	
	2.40E-11	340	1.20E+6	7.80E+4	
	5.10E-11	340	8.00E+5	7.80E+4	
	1.11E-10	340	1.20E+6	7.80E+4	

Pugno model

$$\frac{da}{dN} = C\left(\Delta\sigma\sqrt{\pi\left(a+\left(\frac{\Delta\sigma^{k-m}}{\bar{C}C\pi^{m/2}(m/2-1)}\right)^{1/(m/2-1)}\right)}\right)^m$$

	C	m	$\bar{C}$ [MPa]	k	R	
Steel 1045	8.20E-13	3.5	1.32E+36	11.11	0	[29]

Duggan model

$$\frac{da}{dN} = \frac{1}{\varepsilon'_f}\left[\frac{2\sqrt{\pi/32}}{\sigma'_f E(K_{IC}-K_{max})\left(1-\frac{\Delta K}{K_{IC}}\right)}\right]^{(1/\varepsilon'_f)}\cdot\Delta K^{(2/\varepsilon'_f)}$$

	E [GPa]	σ'_f [MPa]	ε'_f	K_{IC} [MPa.m$^{1/2}$]	R	
2024-T3	70.3	835	0.17	30.0	0.5	[21] [30] [31] [32] [33] [34] [35] [36] [37]
	73.0	1103	0.58	34.1		
	72.0	850	0.22	36.26		
7075-T6	72.2	776	2.57	22.28		
	71.1	729.62	0.26	33.48		
	71.0	781	0.19	37.04		
6082-T6	64.0	611	1.08	33.1		[38] [39] [40] [41]
	70	487	0.209	34.0		
	73.9	477.2	0.696	21.1		

Pandey model

$$\frac{da}{dN} = \frac{(1-n')\psi}{4EI_{n'}\sigma'_f\varepsilon'_f}\left(\Delta K - \Delta K_{th}(1-R)^\gamma\right)^2$$

	E [GPa]	σ'_f [MPa]	ε'_f	n'	γ	$I_{n'}$	ψ	
2219-T851	71	613	0.35	0.121	0.71	3.02	0.9415	[42]
Steel 8630	207	1986	0.42	0.195	0.71	3.082	0.9479	
Steel 4340	209	1713	0.83	0.146	0.71	3.184	0.9481	

Noroozi model

$$\frac{da}{dN} = C\left[\frac{(K_{max})^p}{(\Delta K)^{1-p}}\right]^\gamma$$

	C	P	γ	
2024-T351	5.43E-13	0.5	10	[43]
	8.72E-12	0.09	10	
	9.13E-10	0.09	2.67	
Steel 4340	5.25E-15	0.5	11.64	
	1.83E-13	0.11	11.64	

Ti-6Al-4V			
	4.25E-11	0.11	2.77
Ti-6Al-4V	4.67E-16	0.5	9.62
	1.88E-13	0.960	9.62
	1.00E-10	0.960	2.53

Shi model

$$\frac{da}{dN} = \frac{(1-n')}{4E\psi\sigma'_f\varepsilon'_f}\left(\Delta K - \Delta K_{th}\right)^2$$

avec ; $\psi = (1+n')\pi$

	E [GPa]	σ'_f	n'	ε'_f	ΔK_{th} [MPa.m$^{1/2}$]	R	
7075-T6	71	781	0.088	0.19	1.98	0.5	[37]
2024-T351	70	738	0.100	0.3	2.68	0.0	
2219-T851	71	613	0.121	0.35	2.7	0.1	
Steel 4340	200	1879	0.123	0.64	4.56	0.7	
Steel 1020	205	815	0.18	0.25	11.6	0.1	
X60	200	720	0.132	0.31	8.0	0.1	

Radon model

$$\frac{da}{dN} = \frac{2^{n'-1}(1-2\upsilon)^2}{4\pi(1+n')}\frac{\left(\Delta K_{eff}^2 - \Delta K_s^2\right)}{\sigma_e^{1-n'}\left(E.\varepsilon_f\right)^{1+n'}}$$

	E [GPa]	υ	n'	σ_e [MPa]	ε_f %	ΔK_{th} [MPa.m$^{1/2}$]	R	
2024-T351	70	0.32	0.1	403	19	2.68	0.3	[44] [45] [46] [47] [48] [49] [16][5] [50][38] [51][42] [43] [52] [37] [53] [54]
	72.4			352	18	2.1	-1	
	74	0.33	0.09	363	12.5	2.4	0.2	
	73.0		0.065	379	28	2.1	0.3	
7075-T6	72.2		0.096	512		2.3	0.1	
	71	0.32	0.088	468.85		1.98	0.5	
	70.6		0.062	533	41	1.23	0.7	
	71		0.19	469	41	1.0034	-1	
Steel 4043	209	0.33	0.146	724	14.5	2.6509	-1	
	200		0.14	758	84	5.26	0.1	
	207		0.131	1103	56	3.66	0.5	
	200	0.3	0.123	889.32		4.56	0.7	

Musuva model

$$\frac{da}{dN} = \frac{2^{n'+1}}{4E^{n'}}\frac{\Delta J_{eff} - \Delta J_s}{I_n\left(\varepsilon_f\right)^{n'+1}\left(\sigma_e\right)^{n'-1}}$$

	E [GPa]	υ	n'	σ_e [MPa]	ε_f %	$I_{n'} = \pi(1+n')/(1-2\upsilon)^2$	
Steel 4340	200	0.33	0.123	1039	14.5	Calculated	[55] [42] [37] [54] [51] [45] [56]
	209	0.33	0.146	724	13.0		
304L	196	0.33	0.111	220	84		
	193	0.33	0.341	238	83		
7075-T6	71	0.32	0.088	469			
	70.6	0.32	0.062	540	41		
2024-T351	70	0.32	0.1	403.46	19		
2024 T3	73.1	0.33	0.042	445	20		

All these models cannot be applied in a general way; each of them describes a given situation and becomes unsuitable as soon as a parameter of the experience varies and affecting the fatigue life prediction. However, to find a good results from a model, it is necessary to consider the influence of the intrinsic (Young's modulus, grain size, elastic limit, toughness, etc.) and extrinsic (dimensions of the specimen, and environmental effects, etc.) on the velocity of fatigue crack propagation.

This work aims to develop a Graphical User Interface (GUI) under Matlab which would allow the parametric studies on fatigue life prediction and fatigue crack propagation using different phenomenological models such as those of Paris, Walker and Forman. Also, the novel model proposed by the authors to take into account the influence of hardening parameters.

MODEL PROPOSED

No model for fatigue crack growth described in literature (Table 1) [57], [58] can be applied in a general way but as these models explicate a given situation and become unsuitable as soon as there is any variability of experimental parameters. Therefore, in order to derive reliable results from a model, it is necessary to take into account the influence of both different extrinsic parameters (geometrical and loading) and intrinsic parameters (material properties) on the fatigue crack growth. Then, the choice of model will depend on the effect of certain parameters and stages of cracking. For example, the Forman model considers the influence of the toughness (or hardness K_{IC}) of materials and the last two stages of cracking.

The authors have developed a new model for fatigue crack propagation as a function of hardening parameters (K', n') detailed below:

The relation of Ramberg-Osgood describes the cyclic plastic strain as a function of nominal stress (σ) with cyclic parameters (K', n'):

$$\frac{\Delta \varepsilon_p}{2} = \left(\frac{\Delta \sigma}{2.K'} \right)^{1/n'} \tag{1}$$

The applied nominal stress amplitude is determined as:

$$\Delta \sigma = \frac{\Delta K}{\sqrt{\pi \cdot a}} \tag{2}$$

By substitution, the Ramberg-Osgood relationship is obtained that expresses plastic strain as a function of the stress intensity factor:

$$\frac{\Delta \varepsilon_p}{2} = \left(\frac{\Delta K}{2.K' \sqrt{\pi \cdot a}} \right)^{1/n'} \tag{3}$$

Also:

$$\Delta K = 2.K' \sqrt{\pi \cdot a} \left(\frac{\Delta \varepsilon_p}{2} \right)^{n'}. \tag{4}$$

Based on this relation and the Paris model, we have developed a model that expresses the fatigue crack propagation velocity as a function also of cyclic hardening parameters, defined as follows:

$$\frac{da}{dN} = C\left(2.K'\sqrt{\pi \cdot a}\left(\frac{\Delta\varepsilon_p}{2}\right)^{n'}\right)^m \qquad (5)$$

By integrating equation (1), the number of cycles is given by:

$$N_f = \int_{a_i}^{a_f} \frac{1}{C\left(2.K'\sqrt{\pi \cdot a}\left(\frac{\Delta\varepsilon_p}{2}\right)^{n'}\right)^m} \, da \qquad (6)$$

GRAPHICAL USER INTERFACE (GUI)
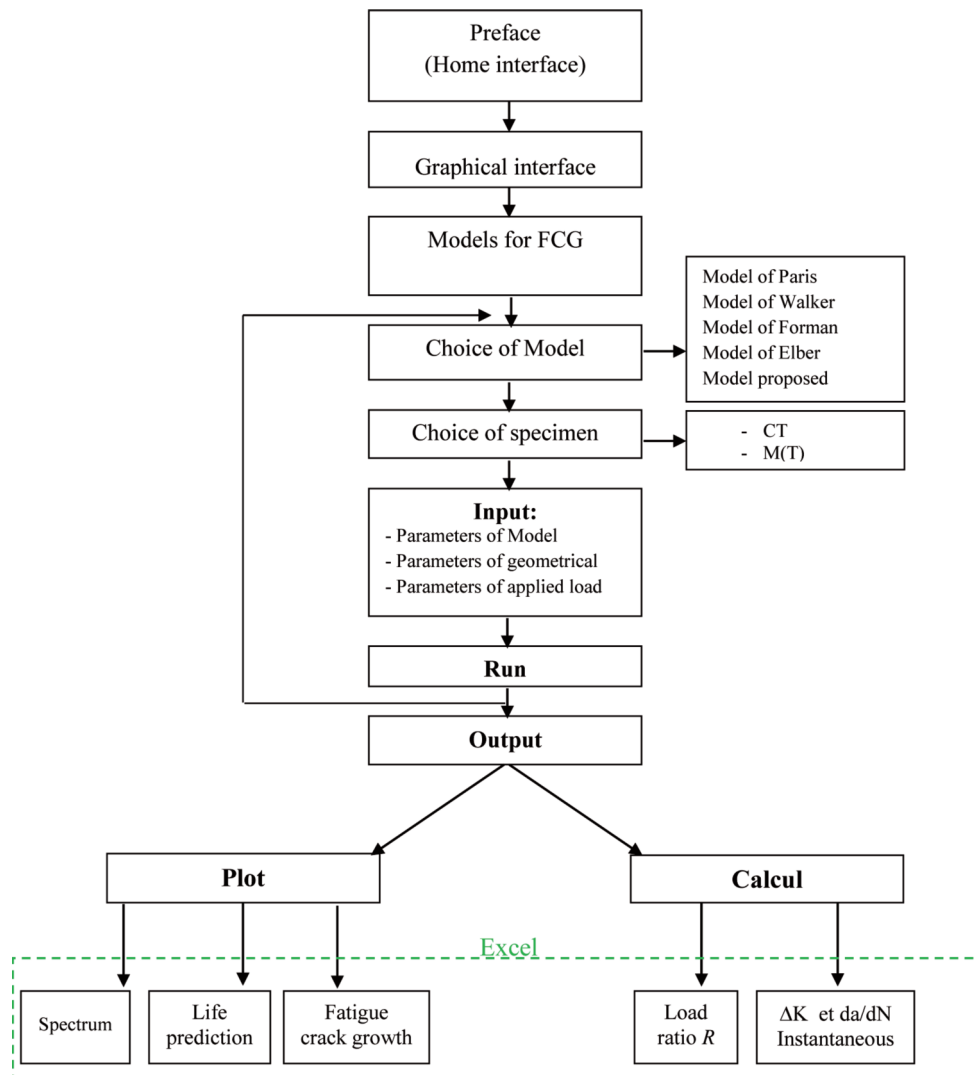
Figure 1. Methodology of Graphical User Interface (GUI).

A Graphical User Interface (GUI) under Matlab for predicting fatigue life was developed. The influence of different extrinsic (geometric and loading) and intrinsic (material properties) parameters on the fatigue life was taken into account. The fatigue crack growth models used were those developed by Paris, Elber, Walker, Forman and model proposed here. Matlab (Matrix Laboratory) software is an interactive digital computing system that has a large number of functions, a programming language and graphical visualization tools.

A Graphical User Interface under Matlab is a set of graphical elements allowing users to interact with parts of programs by displaying information (texts, graphics, images, curves, etc.) and by triggering actions following events; mouse click, mouse movement, keyboard input, etc.

An example of a user interface is a window linked to a figure and the objects it can contain (menus, buttons, axes). To develop the Graphical User Interface, we have developed an organization chart in which we have the operating principles and the different stages of the creation of this interface (Figure 1).

Creation steps

Building the Graphical User Interface was accomplished by several stages consisting in programming the script with file type (file.m) programmed in Matlab and grouped in the same folder. The detail of each step is given by the below:

1. **Preface** is a window which displays the home page for a duration of ten seconds. It carries personal information of the creator of the interface (Name, Title, University, Year, etc.) (Figure 2).
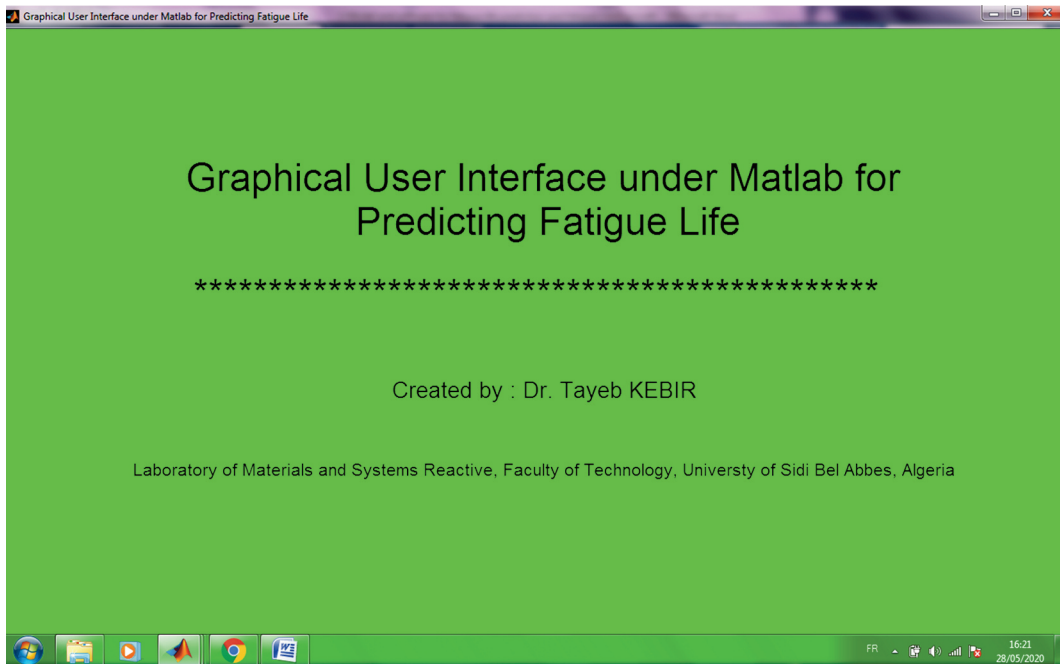
Figure 2. Screen capture of home page.

2. **Graphical interface:** if you run the preface program in Matlab, first the home page is fully lit then goes out after 10 seconds, after the interface window will start automatically and display a window where different cracking models (Paris, Walker, Forman, Elber and Model proposed) appear as shown in Figure 3.
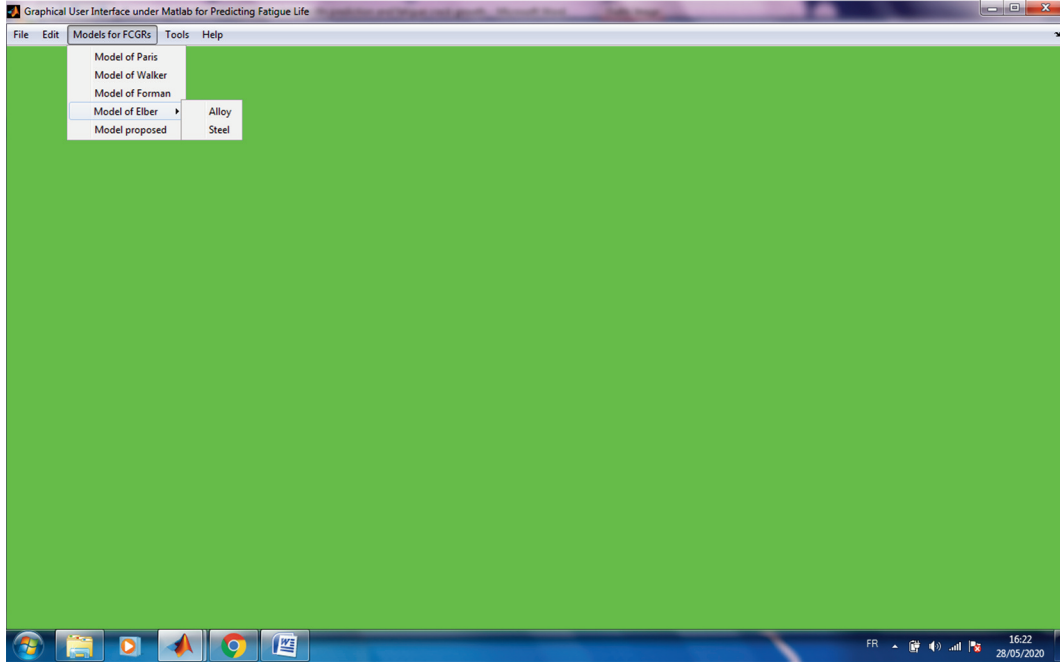
Figure 3. Screen capture of graphical user interface.

3. **FCG Models:** The fatigue life estimate is obtained from the models for crack propagation presented in Table 2. For each model there is a script file programmed and developed under Matlab. The choice of model will depend on the effect of certain parameters and the stages of cracking. For example, the use of the Forman model allows taking into account the toughness of the material and the last two stages of cracking.

4. **Choice of specimen:** The stress intensity factor depends both on the specimen relative to its geometric design, and loading, and on the crack relative to its size (a). It is expressed in MPa.m$^{1/2}$.

In this study, we used two types of specimen C(T) and M(T) [2], see Figure 4. The expressions of the amplitude of the stress intensity factor are presented by the relations (7) and (8) respectively.

$$\Delta K = \frac{\Delta P}{B}\sqrt{\frac{\pi\alpha}{2w}\sec\frac{\pi\alpha}{2}} \quad \text{with } \alpha = (2a/w) \quad \text{For M(T)} \tag{7}$$

$$\Delta K = \frac{\Delta P}{B}\sqrt{\pi a}\,f(\alpha') \quad \text{with } \alpha' = (a/w) \quad \text{For C(T)} \tag{8}$$

$$f(\alpha') = \frac{2+\alpha'}{(1-\alpha')^{3/2}}\left[0.886+4.64(\alpha')-13.32(\alpha')^2+14.72(\alpha')^3-5.6(\alpha')^4\right] \quad (9)$$

Where: B and w are the width and thickness of the specimen, respectively; the amplitude of the mechanical loading is given by $\Delta P = (P_{max} - P_{min})$.

These two equations are thus programmed under Matlab script (file.m) and integrated into the files of the cracking models.
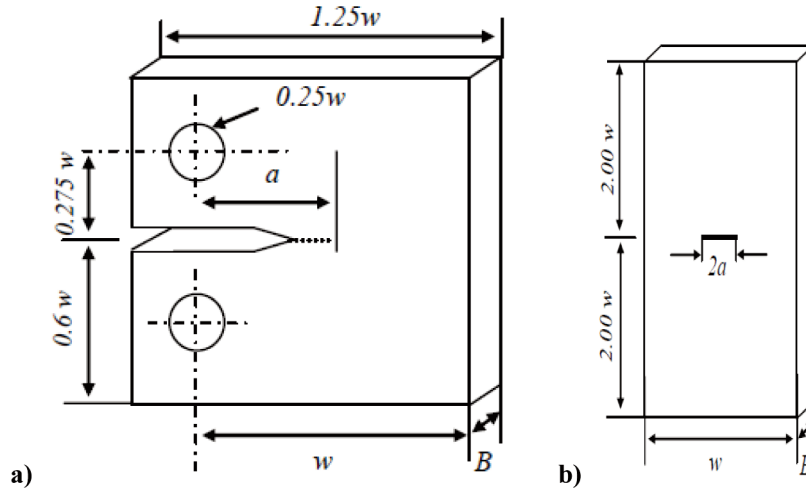
Figure 4. Design of specimen, a) C(T), b) M(T).

5. **Input parameters:** This step follows the previous steps and will depend on the execution of the previous programs. The correct execution (or run) of these programs (choice of model, choice of specimen) results in the display of a window with the chosen model, the geometric parameters (B and w), the loadings (Frequency f, maximum load P_{max} and minimum P_{min}) and the command buttons (Spectrum, Life, Speed, Return, etc.). All of these steps are given in Figure 5. The input values are obtained using the experimental results [3].

6. **Output:** When the values of these parameters are entered (Input), the command buttons (Spectrum, Life, Speed, Calculate) will allow the user to view the results in the form of curves or values, also we can export the following results data from excel file:
   - Life prediction curve,
   - Fatigue crack growth curve,
   - Value of the final cycle and the amplitude of the stress intensity factor with speed of cracking at a given crack size, see Figure 5.
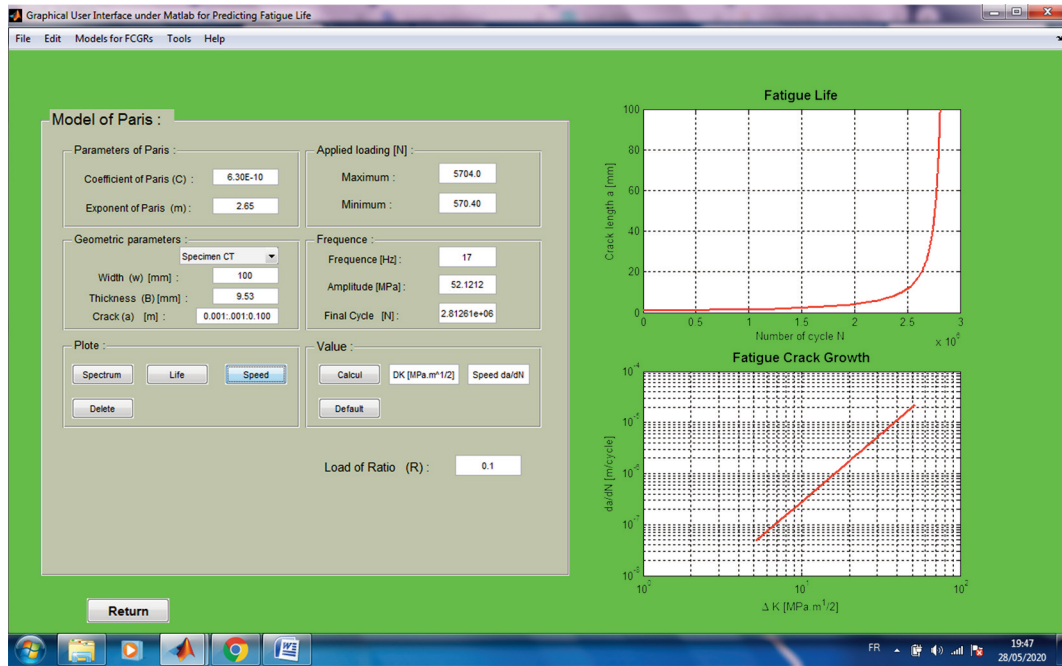
Figure 5. Screen capture of input parameters, case of Paris's Model.

APPLICATION

The creation of this Graphical User Interface allowed us to make parametric studies on fatigue crack propagation, using different phenomenological models such as those of Paris, Walker, Forman and the model proposed here, see Table 2. Also, fatigue life estimation is obtained from the models for fatigue crack propagation presented in Table 2. For this purpose, we carried out four applications that are classified according to the four cracking models used. The development of the integral under Matlab makes it possible to calculate fatigue lifetime N_f:

Table 2. Models for fatigue crack growth.

Models	Fatigue life prediction
Paris: $\dfrac{da}{dN} = C\left(\Delta K\right)^m$	$N_f = \displaystyle\int_{a_i}^{a_f} \dfrac{1}{C\left(\Delta K\right)^m}\, da$
Walker: $\dfrac{da}{dN} = \dfrac{C_0}{\left(1-R\right)^{m_0(1-\gamma)}}\left(\Delta K\right)^{m_0}$	$N_f = \displaystyle\int_{a_i}^{a_f} \dfrac{\left(1-R\right)^{m_0(1-\gamma)}}{C\left(\Delta K\right)^{m_0}}\, da$
Forman: $\dfrac{da}{dN} = \dfrac{C'\left(\Delta K\right)^{m'}}{\left(1-R\right)\left(K_{\max} - K_{IC}\right)}$	$\dfrac{da}{dn} = C\left(2.K'\sqrt{\pi \cdot a}\left(\dfrac{\Delta\varepsilon_p}{2}\right)^{n'}\right)^m$
Model proposed: $\dfrac{da}{dn} = C\left(2.K'\sqrt{\pi \cdot a}\left(\dfrac{\Delta\varepsilon_p}{2}\right)^{n'}\right)^m$	$N_f = \displaystyle\int_{a_i}^{a_f} \dfrac{1}{C\left(2.K'\sqrt{\pi \cdot a}\left(\dfrac{\Delta\varepsilon_p}{2}\right)^{n'}\right)^m}\, da$

Application 1, using the Paris model

In this application, the influence of the Paris exponent m is studied with the use of two different aluminum alloys 2024-T3 and 7075-T6 whose different parameters of the Paris law are given in Table 3. These parameters were obtained from experimental results obtained by Forth et al. [3] under boundary conditions of specimen M(T) and applied loading (P_{max} and P_{min}) given in Table 4.

Table 3. The Paris' law parameters.

Alloys	C [mm/cycle]	m	Ref.
2024-T3	2.89E-9	3.037	[3]
7075-T6	1.31E-9	2.902	

Table 4. Boundary conditions.

Alloys	W [mm]	B [mm]	P_{max} [N]	P_{min} [N]	R	Ref.
2024-T3	100.35	9.53	5704	570.4	0.1	[3]
7075-T6	102.03	3.18	1902	190.2	0.1	
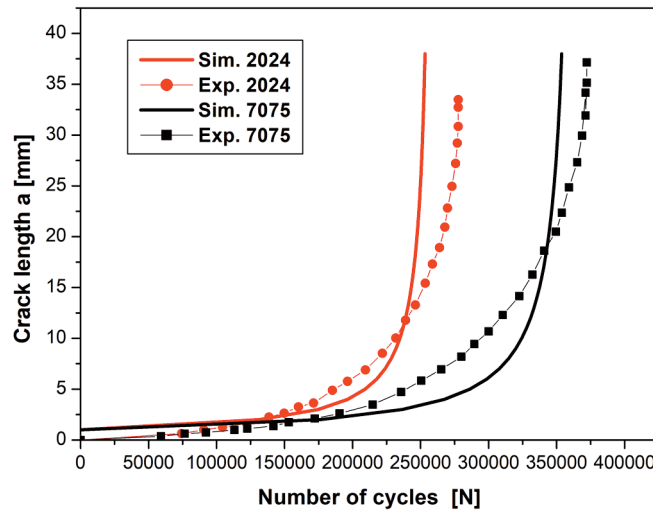
Figure 6. Crack length as a function of number of cycles
with experimental results [3].

The results expressed in fatigue life prediction of alloys 2024 and 7075 show a good agreement with the experimental study carried out by Forth et al. [3] and are presented in Figure 6. Figure 6 shows the evolution of crack length (a) as a function of number of cycles (N). It can be seen that under these boundary conditions of specimen and loading applied, the lifetime for alloy 7075 is 350.000 cycles, while that for alloy 2024 is 250.000 cycles. It is shorter life with a shift of 100000 cycles. Indeed, the exponent m which represents the slope of the cracking curve is much larger for 2024 alloy

($m = 3.037$) hence a much higher crack propagation rate for the same length (a) or the same (K). This is illustrated by Figure 7, which shows the evolution of fatigue crack propagation (da/dN) as a function of the stress intensity factor (K). It can be concluded that the effect of the exponent on the cracking curves is very significant. When the Paris exponent (m) increases, the crack propagation curve shifts to the left and the speed (da/dN) of fatigue crack growth increases.
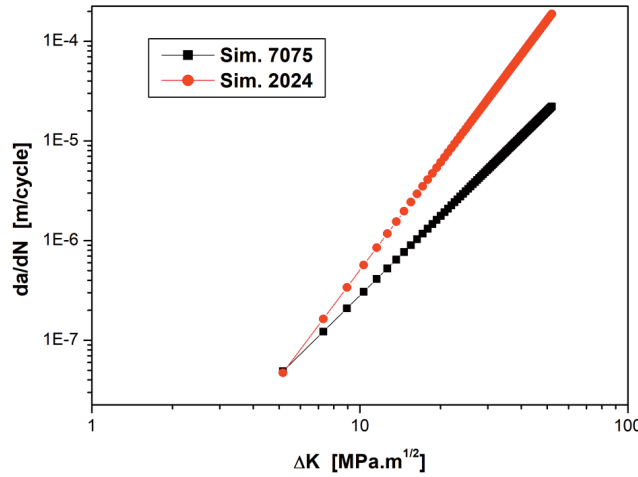

Figure 7. Fatigue crack growth rate
versus stress intensity factor K.

Application 2, using the Walker model

In the second application, we were interested in the influence of the load ratio R using the Walker model. In this work, the material studied was Aluminum alloy 2024, whose properties are presented in Table 5. The boundary conditions of specimen (CT) and loading are given in Table 6.

Table 5. The Walker's law parameters.

Alloy	C_0 [mm/cycle]	m_0	y	Ref.
2024-T3	2.66E-8	3.9	0.564	[18], [59]

Table 6. Boundary conditions of 2024-T3.

Alloy	B [mm]	W [mm]	P_{max} [N]	P_{min} [N]	R
2024-T3	75	6	5000	500	0.1
			5000	1500	0.3
			5000	2500	0.5

Figure 8 shows the evolution of fatigue crack length as a function of number of cycles relative to the variability of load ratio R. It can be observed that the increase in load ratio R results in a decrease in fatigue lifetime.
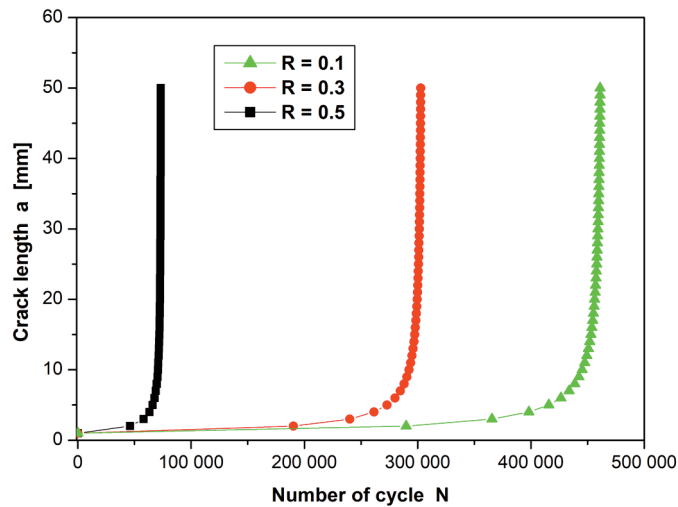
Figure 8. Evolution of fatigue crack length as a function
of number of cycles for 2024.

Figure 9 shows the fatigue crack propagation rate as a function of stress intensity factor (K). The influence of load ratio R is well noticed for the fatigue crack growth, an increase in load ratio R causes a decrease in the fatigue lifetime prediction [45], [60].
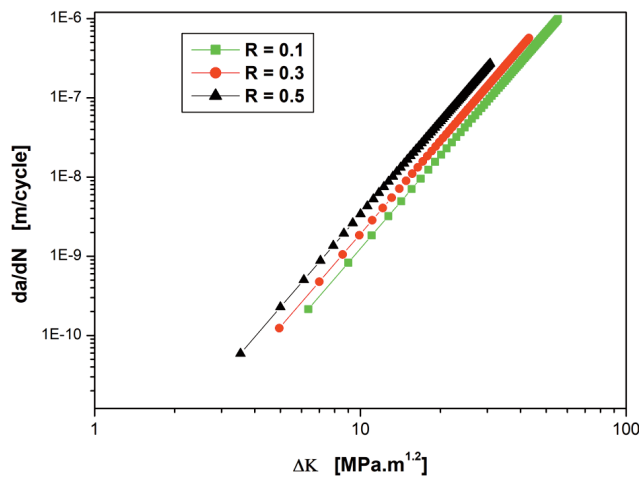

Figure 9. Fatigue crack growth rate
versus stress intensity factor K for 2024.

Application 3, using the Forman model

In this application, the influence of the hardness (or toughness K_{IC}) of a material is highlighted. Forman's model is expressed as a function of toughness (K_{IC}), and takes into account the domain three for fatigue crack growth, when the amplitude of the intensity factor tends towards the amplitude of the critical stress intensity factor represented by the hardness (or toughness K_{IC}) of material.

The material used was alloy 2024-T3 whose properties are presented in Table 7. The boundary conditions of the test specimen and loading applied are given in Table 8.

Table 7. The Forman law parameters.

Alloy	C' [mm/cycle]	m'	K_{IC} [MPa.m$^{1/2}$]	Ref.
2024-T3	6.30E-1	02.65	35	[5]

Table 8. Boundary conditions of 2024-T3.

Alloy	B [mm]	W [mm]	P_{max} [N]	P_{min} [N]	R
2024-T3	75	6	5704	570.4	0.1

The results obtained from the experimental tests described in the literature give different values with errors [5], [35]. Hence we proposed variability on the values obtained from the hardness (32, 35 and 38 MPa.mm$^{1/2}$). Given these results, the calculations obtained by Graphical User Interface (GUI) under Matlab software were performed by varying toughness (K_{IC}).

Figure 10 shows the evolution of the fatigue crack length as a function of number of cycles under the influence of variability of toughness (K_{IC}). Despite small difference in the toughness values, the latter has a great impact on the fatigue crack growth of the material. Indeed, the fatigue lifetime prediction is all the more important when toughness increases. This is to say that a material with high toughness is more resistant to fatigue crack propagation [5], [35].
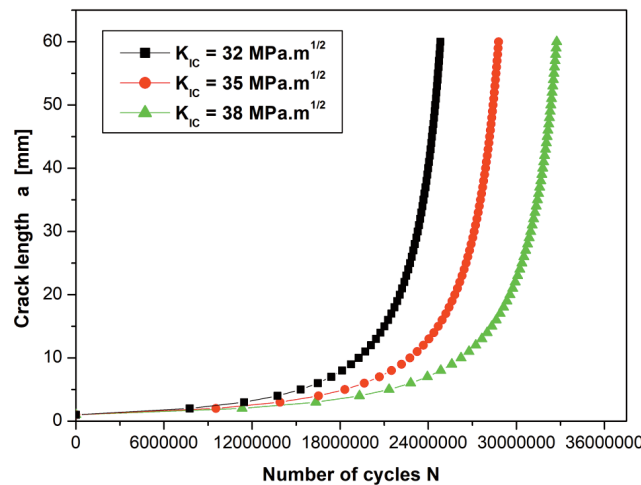
Figure 10. Evolution of fatigue crack length
versus number of cycles for 2024.

Figure 11 shows the evolution of the fatigue crack growth rate (da/dN) as a function of the stress intensity factor (K) for different values of K_{IC}. The fatigue crack propagation curve shifts to the right as toughness increases meaning a slower speed of fatigue crack growth and a better fatigue life prediction.
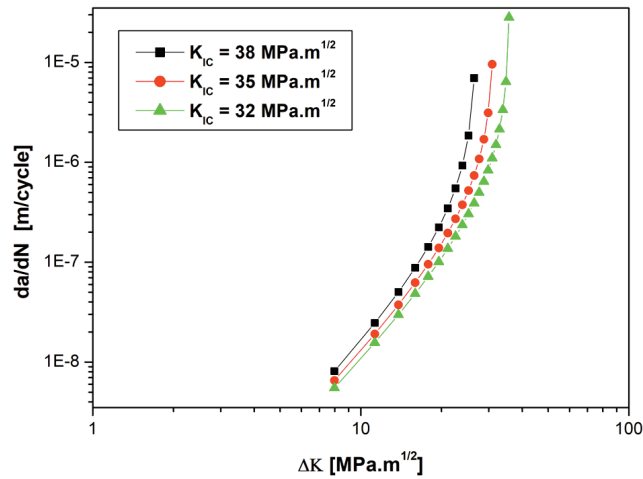
Figure 11. Fatigue crack growth rate
versus of stress intensity factor K.

Application 4, using the proposed model

The model proposed presents fatigue crack growth as a function of cyclic hardening parameters (K' and n'). It allowed us to do the parametric studies of fatigue life prediction and fatigue crack growth as affected by cyclic hardening parameters, using the Graphical Interface, see Figure 12.
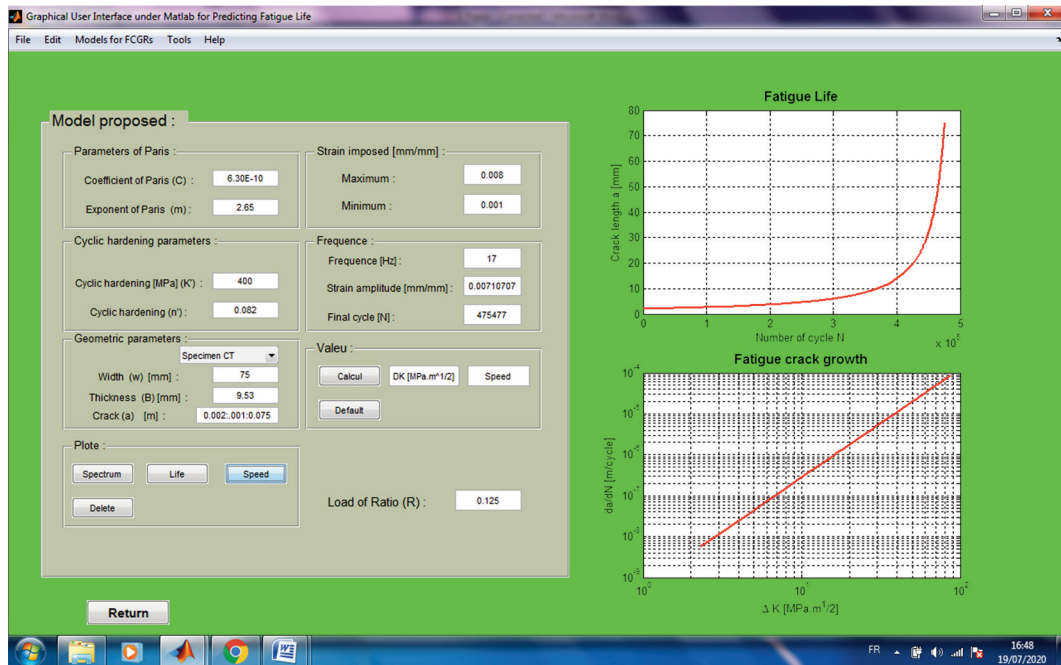

Figure 12. Screen capture of input parameters, case of model proposed.

For this application, we used 2024-T3Aluminum Alloy with properties of cyclic hardening (K', n') and parameters of Paris (C, m) as shown in Table 9. Table 10 presents the boundary conditions for the test specimen and the loading applied. The variability

of parameters cyclic hardening proposed when all the values of material properties obtained by experimental tests are not exact values, these are lacking reliability, needs us to studies their effect on fatigue life prediction using the manipulator of our Graphical Interface (Figure 3).

Table 9. The parameters of Model proposed.

Alloy	C' [mm/cycle]	m'	K' [MPa]	n'	Ref.
2024-T3	6.30E-10	2.65	420	0.072	[2]
			400	0.082	
			440	0.092	

Table 10. Boundary conditions of 2024-T3.

Alloy	B [mm]	W [mm]	ε_{max} [%]	ε_{min} [%]	R
2024-T3	75	9.53	0.80	0.1	0.1

Figure 13 presents the evolution of crack length versus the number of cycles have the same trend comparatively for three variability of the hardening exponent (n'), are shown also that the decrease in cyclic hardening exponent (n'), decreases the fatigue life prediction for 2024 T3 Al-alloy. This decrease in fatigue life is due to reduced fatigue resistance and the size of the plastic zone. The curve initially starts as a straight line with a small slope. This is the elastic region. In this region, the plastic strain is absent and crack length (a) slightly increases with the number of cycles N. As plastic strains evolve with increasing stress (larger crack length) beyond the yield point at some point on the crack front, the graphs turn upwards. The hardening exponent (n') governs the magnitude of the plastic strains and, therefore, the change of crack length depending on the number of cycles [2], [6].
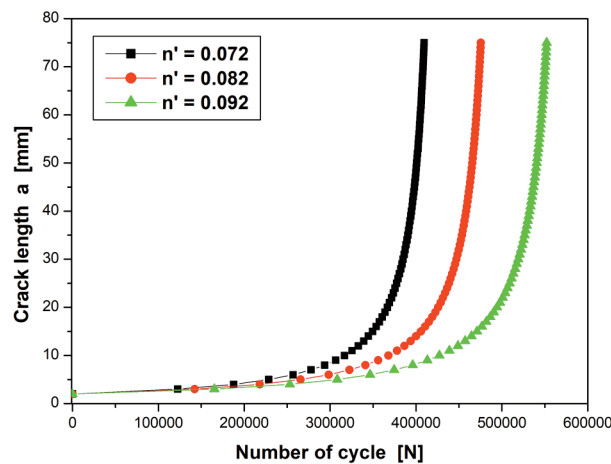

Figure 13. Crack length versus number of cycles for 2024-T3, under variability of cyclic hardening (n').

Figure 14 shows the evolution of the crack length versus the number of cycles under the variability of the cyclic hardening coefficient (K') for 2024-T3 alloy studied. It can be observed that when the number of cycle increases, the crack length increases too, irrespective of the value of cyclic hardening (K'), Also, increasing cyclic hardening (K') leads to decreasing the fatigue life prediction.
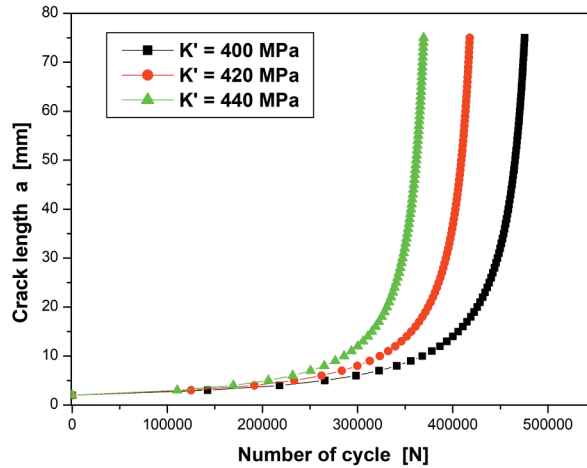

Figure 14. Crack length versus the number of cycles for 2024-T3,
under variability of cyclic hardening (K').

Figure 15 displays the fatigue crack growth rate as a function of the range of the stress intensity factor for three different values of cyclic hardening (n'). The effect to variability it seems clearly suitable thus the velocity to fatigue crack propagation increases when the cyclic hardening decreases.
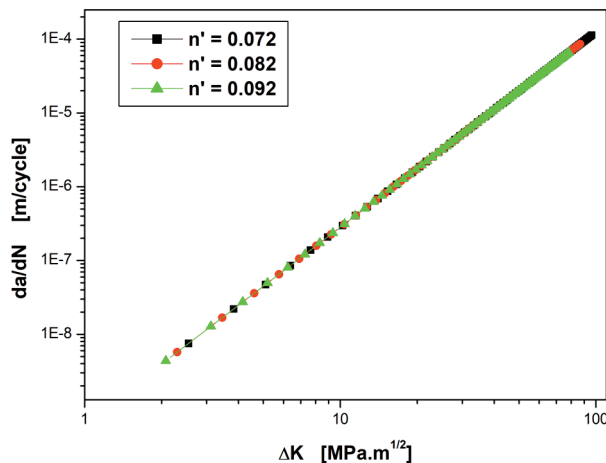

Figure 15. Fatigue crack growth versus the (K) for 2024-T3,
under variability of cyclic hardening (n').

The variability of the cyclic hardening coefficient (K') on the evolution of the fatigue crack propagation for alloy 2024-T3 is visible in Figure 16. It can be seen that the fatigue crack propagation increases when the cyclic hardening coefficient increases.
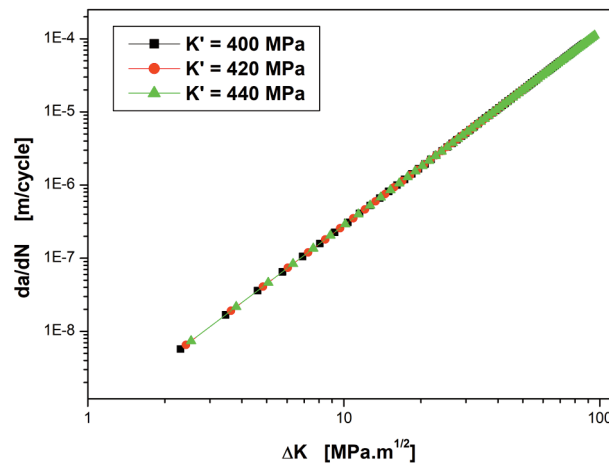
Figure 16. Fatigue crack growth versus the (K) for 2024-T3, under variability of cyclic hardening coefficient (K').

CONCLUSION

The objective of this work was to create a Graphical User Interface (GUI) under Matlab enabling parametric studies of fatigue prediction and fatigue crack growth using four models of fatigue crack growth (Paris, Walker, Forman and model proposed). The main factors studied were the exponent m, the load ratio R, the toughness K_{IC} and the cyclic hardening (K', n'). Based on the analysis of the Graphical User Interface and performed calculations, the following conclusions were reached:

- The fatigue crack propagation curve shifts to the left when the Paris exponent m increases and leads to decreasing the fatigue lifetime prediction.
- The load ratio R has a great influence on fatigue crack growth; fatigue life decreases when the load of ratio R increases,
- A material with high toughness is more resistant to fatigue crack propagation.
- The effect to variability it seems clearly suitable thus the velocity to fatigue crack propagation increases when the cyclic hardening exponent decreases.
- The cyclic hardening exponent decrease, decreasing the fatigue life prediction
- The influence of the cyclic hardening (K') is well marked on the fatigue prediction. Increasing values of cyclic hardening (K') lead to decreasing fatigue life prediction. Therefore, fatigue crack propagation increases when the cyclic hardening coefficient increases.

The Graphical User Interface makes it possible to identify the parameters (material properties, specimen dimensions and loading applied) that affect fatigue life prediction and fatigue crack growth, thus enabling performing a reliable parametric study.

REFERENCES

[1]   Grasso, M., Penta, F., Pinto, P. and Pucillo, G.P. (2013). A four-parameters model for fatigue crack growth data analysis. *Frat. ed Integrita Strutt.*, vol. 26, pp. 69–79. DOI: 10.3221/IGF-ESIS.26.08.

[2]   Kebir, T., Benguediab, M. and Imad, A. (2017). A Model for Fatigue Crack Growth in the Paris Regime under the Variability of Cyclic Hardening and Elastic Properties. *Fatigue of Aircraft Structure*, vol. 2017, no. 9, pp. 117–135. DOI: 10.1515/fas-2017-0010.

[3]   Forth, S.C., Wright, C.W. and Johnston, W.M. (2005). *7075-T6 and 2024-T351 aluminum alloy fatigue crack growth rate data*. Virginia: NASA Langely Research Center. (NASA/TM-2005-213907), pp. 1–19.

[4]   Ould Chikh, B., Imad, A. and Benguediab, M. (2008). Influence of the cyclic plastic zone size on the propagation of the fatigue crack in case of 12NC6 steel. *Computational Materials Science*, vol. 43, pp. 1010–1017. DOI: 10.1016/j.commatsci.2008.02.019.

[5]   Kim, J.-K. and Shim, D.-S. (2000). The variation in fatigue crack growth due to the thickness effect. *International Journal of Fatigue*, vol. 22, pp. 611–618. DOI: 10.1016/S0142-1123(00)00032-3.

[6]   Kebir, T., Benguediab, M. and Imad, A. (2017). Influence of the variability of the elastics properties on plastic zone and fatigue crack growth. *Mechanics and Mechanical Engineering*, vol. 21, no. 4, pp. 919–934.

[7]   Paul, S.K. and Tarafder, S. (2013). Cyclic plastic deformation response at fatigue crack tips. *International Journal of Pressure Vessels and Piping*, vol. 101, pp. 81–90. DOI: 10.1016/j.ijpvp.2012.10.007.

[8]   Jean-Christophe, L.R. (1999). *Étude du comportement et de L'endommagement en fatigue d'un acier inoxydable austéno-ferritique moulé Vieilli*. PhD Thesis, Ecole Centrale de Paris.

[9]   Prasad, K., Kumar, V., Bhanu Sankara Rao, K. and Sundararaman, M. (2016). Effects of crack closure and cyclic deformation on thermomechanical fatigue crack growth of a Near α Titanium Alloy. *Metallurgical and Materials Transactions A*, vol. 47, pp. 3713–3730. DOI: 10.1007/s11661-016-3482-y.

[10]   Borges, M.F., Antunes, F.V., Prates, P.A. and Branco, R. (2020). A numerical study of the effect of isotropic hardening parameters on mode I fatigue crack growth. *Metals*, vol. 10, no. 2, p. 177. DOI: 10.3390/met10020177.

[11]   Borges, M.F., Antunes, F.V., Prates, P., Branco, R., Vasco-Olmo, J.M. and Díaz, F.A.(2020). Model for fatigue crack growth analysis. *Procedia Structural Integrity*, vol. 25, no. 2020, pp. 254–261. DOI: 10.1016/j.prostr.2020.04.030.

[12]   Alaoui, A.E.M. (2005). *Influence du chargement sur la propagation en fatigue de fissures courtes dans un acier de construction navale*. Thesis Doctor, University of Metz.

[13]   Yahiaoui, B. and Petrequin, P. (1974). Etude de la propagation de fissures par fatigue dans des aciers inoxydables austénitiques à bas carbone du type 304L et 316L. *Rev. Phys. Appl. (Paris)*, vol. 9, no. 4, pp. 683–690. DOI: 10.1051/rphysap:0197400904068300.

[14]   Singh, P.J., Achar, D.R.G., Guha, B. and Nordberg, H. (2003). Fatigue life prediction of gas tungsten arc welded AISI 304L cruciform joints with different LOP sizes. *International Journal of Fatigue*, vol. 25, no. 1, pp. 1–7. DOI: 10.1016/S0142-1123(02)00067-1.

[15]   Ould Chikh, E.B., Nianga, J.M., Imad, A. and Benguediab, M. (2007). Correlation between the coefficients C and m of paris law for fatigue crack growth and the effect of the variability of these parameters on the prediction of the lifetime in the case of heat treated 12NC6 steel. CFM 2007 − 18ème Congrès Français de Mécanique, Aug 2007, Grenoble, France. From https://hal.archives-ouvertes.fr/hal-03362074.

[16]   Xiang, Y., Lu, Z. and Liu, Y. (2010). Crack growth-based fatigue life prediction using an equivalent initial flaw model. Part I: Uniaxial loading. *International Journal of Fatigue*, vol. 32, no. 2, pp. 341–349. DOI: 10.1016/j.ijfatigue.2009.07.011.

[17] Mann, T. (2006). *Fatigue assessment methods for welded structures and their application to an aluminium T-joint*. PhD Doctor, University of science and technology, Norwegian.

[18] Melson, J. H. (2014). *Fatigue crack growth analysis with finite element methods and a monte carlo simulation*. Thesis Master, Faculty of the Virginia Polytechnic Institute.

[19] Mann, T. (2007). The influence of mean stress on fatigue crack propagation in aluminium alloys. *International Journal of Fatigue*, vol. 29, no. 8, pp. 1393–1401. DOI: 10.1016/j.ijfatigue.2006.11.010.

[20] Correia, J.A.F.O. et al. (2016). Modified CCS fatigue crack growth model for the AA2019-T851 based on plasticity-induced crack-closure. *Theoretical and Applied Fracture Mechanics*, vol. 85, pp. 26–36. DOI: 10.1016/j.tafmec.2016.08.024.

[21] Forman, R.G., Shivakumar, V., Cardinal, J.W., Williams, L.C. and McKeighan, P.C. (2005). *Fatigue crack growth database for damage tolerance analysis*. Springfield, Virginia: NTIS. (DOT/FAA/AR-05/15).

[22] Mohanty, J.R., Verma, B.B. and Ray, P.K. (2009). Prediction of fatigue crack growth and residual life using an exponential model: Part I (constant amplitude loading). *International Journal of Fatigue*, vol. 31, pp. 418–424. DOI: 10.1016/j.ijfatigue.2008.07.015.

[23] Johan Singh, P., Mukhopadhyay, C., Jayakumar, T., Mannan, S. and Raj, B. (2007). Understanding fatigue crack propagation in AISI 316 (N) weld using Elber's crack closure concept: Experimental results from GCMOD and acoustic emission techniques. *International Journal of Fatigue*, vol. 29, no. 12, pp. 2170–2179. DOI: 10.1016/j.ijfatigue.2006.12.013.

[24] Alrubaie, K., Barroso, E. and Godefroid, L. (2006). Fatigue crack growth analysis of pre-strained 7475–T7351 aluminum alloy. *International Journal of Fatigue*, vol. 28, no. 8, pp. 934–942. DOI: 10.1016/j.ijfatigue.2005.09.008.

[25] Wang, Y., Cui, W., Wu, X., Wang, F. and Huang, X. (2008). The extended McEvily model for fatigue crack growth analysis of metal structures. *International Journal of Fatigue*, vol. 30, no. 10–11, pp. 1851–1860. DOI: 10.1016/j.ijfatigue.2008.01.014.

[26] Božić, Ž. Mlikota, M. Schmauder, S. (2011). Application of the ΔK, ΔJ and ΔCTOD parameters in fatigue crack growth modelling. *Tehnicki Vjesnik*, vol. 18, no. 3, pp. 459–466.

[27] Klingbeil, N.W. (2003). A total dissipated energy theory of fatigue crack growth in ductile solids. *International Journal of Fatigue*, vol. 25, pp. 117–128. DOI: 10.1016/S0142-1123(02)00073-7.

[28] Yao, Y., Fine, M.E. and Keer, L.M. (2007). An energy approach to predict fatigue crack propagation in metals and alloys. *International Journal of Fracture*, vol. 146, no. 3, pp. 149–158. DOI: 10.1007/s10704-007-9156-4.

[29] Pugno, N., Ciavarella, M., Cornetti, P. and Carpinteri, A. (2006). A generalized Paris' law for fatigue crack growth. *Journal of the Mechanics and Physics of Solids*, vol. 54, no. 7, pp. 1333–1349. DOI: 10.1016/j.jmps.2006.01.007.

[30] Fu, D.L., Zhang, L. and Cheng, J. (2006). An energy-based approach for fatigue crack growth. *Key Engineering Materials*, vol. 324–325, pp. 379–382. DOI: 10.4028/www.scientific.net/KEM.324-325.379.

[31] Karakaş Ö. and Szusta, J. (2016). Monotonic and low cycle fatigue behaviour of 2024-T3 aluminium alloy between room temperature and 300°C for designing VAWT components. *Fatigue & Fracture of Engineering Materials & Structures*, vol. 39, no. 1, pp. 95–109. DOI: 10.1111/ffe.12336.

[32]   Schreurs, P.J.G. (2012). Fracture Mechanics Background. In Stephen W. Freiman and John J. Mecholsky Jr. (Eds.) *The Fracture of Brittle Materials: Testing and Analysis*, Hoboken, NJ, USA: John Wiley & Sons, Inc., pp. 62–63.

[33]   Beden, S.M., Abdullah, S., Ariffin, A.K. and Al-Asady, N.A. (2010). Fatigue crack growth simulation of aluminium alloy under spectrum loadings. *Materials and Design*, vol. 31, no. 7, pp. 3449–3456. DOI: 10.1016/j.matdes.2010.01.039.

[34]   Dimitriu, R.C. and Bhadeshia, H.K.D.H. (2010). Fatigue crack growth rate model for metallic alloys. *Materials and Design*, vol. 31, pp. 2134–2139. DOI: 10.1016/j.matdes .2009.11.019.

[35]   Kumar, S.M., Pramod, R., Kumar, M.E.S. and Govindaraju, H.K. (2014). Evaluation of fracture toughness and Mechanical Properties of Aluminum Alloy 7075, T6 with Nickel Coating. *Procedia Engineering*, vol. 97, pp. 178–185. DOI: 10.1016/j.proeng .2014.12.240.

[36]   Noroozi, A.H., Glinka, G. and Lambert, S. (2008). Prediction of fatigue crack growth under constant amplitude loading and a single overload based on elasto-plastic crack tip stresses and strains. *Engineering Fracture Mechanics*, vol. 75, no. 2, pp. 188–206. DOI: 10.1016/j.engfracmech.2007.03.024.

[37]   Shi, K., Cai, L. and Bao, C. (2014). Crack growth rate model under constant cyclic loading and effect of different singularity fields *Procedia Materials Science*, vol. 3, pp. 1566–1572. DOI: 10.1016/j.mspro.2014.06.253.

[38]   Fatemi, A., Plaseied, A., Khosrovaneh, A.K. and Tanner, D. (2005). Application of bi-linear log-log S-N model to strain-controlled fatigue data of aluminum alloys and its effect on life predictions. *International Journal of Fatigue*, vol. 27, no. 9, pp. 1040–1050. DOI: 10.1016/j.ijfatigue.2005.03.003.

[39]   Ribeiro, A.S., Borrego, L.P., De Jesus, A.M.P. and Costa, J.D.M. (2009). Comparison of the low-cycle fatigue properties betwee the 6082-T6 and 6061-T651 Aluminium Alloys. In *20th International Congress of Mechanical Engineering*. November15-20, Gramado, RS, Brazil.

[40]   Han, J.W., Han, S.H., Shin, B.C. and Kim, J.H. (2012). Fatigue Crack Initiation and Propagation Life of Welded Joints. Key Engineering Materials, vol. 297–300, pp. 781–787. DOI: 10.4028///www.scientific.net/KEM.297-300.781.

[41]   Mrowka, N.G., Sieniawski, J. and Nowotnik, A. (2009). Effect of heat treatment on tensile and fracture toughness properties of 6082 alloy. *Journal of Acheivements in Materials and Manufacturing Engineering*, vol. 32, no. 2, pp. 162–170.

[42]   Pandey, K. and Chand, S. (2003). An energy based fatigue crack growth model. *International Journal of Fatigue*, vol. 25, no. 8, pp. 771–778. DOI: 10.1016/S0142-1123(03)00049-5.

[43]   Noroozi, A., Glinka, G. and Lambert, S. (2007). A study of the stress ratio effects on fatigue crack growth using the unified two-parameter fatigue crack growth driving force. *International Journal of Fatigue*, vol. 29, no. 9–11, pp. 1616–1633. DOI: 10.1016/j. ijfatigue.2006.12.008.

[44]   Radon, J.C. (1982). A model for fatigue crack growth in a threshold region. *International Journal of Fatigue*, vol. 4, no. 3, pp. 161–166. DOI: 10.1016/0142-1123(82)90044-5.

[45]   Noroozi, A., Glinka, G. and Lambert, S. (2005). A two parameter driving force for fatigue crack growth analysis. *International Journal of Fatigue*, vol. 27, no. 10–12, pp. 1277–1296. DOI: 10.1016/j.ijfatigue.2005.07.002.

[46] Benachour, M., Benguediab, M. and Benachour, N. (2013). Notch fatigue crack initiation and propagation life under constant amplitude loading through residual stress field. *Advanced Materials Research*, vol. 682, pp. 17–24. DOI: 10.4028/www.scientific.net/AMR.682.17.

[47] Tschegg, S.E.S. and Mayer, H. (2001). Fatigue and fatigue crack growth of aluminium alloys at very high numbers of cycles. *International Journal of Fatigue*, vol. 23, pp. 231–237. DOI: 10.1016/S0142-1123(01)00167-0.

[48] Benachour, N., Hadjoui, A., Benachour, M. and Benguediab, M. (2011). Stress ratio and notch effect on fatigue crack initiation and propagation in 2024 Al-alloy. *International Journal of Mechanical and Mechatronics Engineering*, vol. 5, no. 7, pp. 1384–1387.

[49] Grasso, M., Iorio, A., Xu, Y., Haritos, G., Mohin, M. and Chen, Y.K. (2017). An analytical model for the identification of the threshold of stress intensity factor range for crack growth. *Advances in Materials Science and Engineering*, vol. 2017, 3014172. DOI: 10.1155/2017/3014172.

[50] Forth, S.C., Newman, J.C. and Forman, R.G. (2002). Generating fatigue crack growth thresholds with constant amplitude loads. *Fatigue*, pp. 1–8. https://ntrs.nasa.gov/api/citations/20030014136/downloads/20030014136.pdf

[51] Colin, J. (2010). *Deformation history and load sequence effects on cumulative fatigue damage and life predictions*. Thesis Doctor, University of Toledo Digital Repository.

[52] Anand, L. and Parks, D.M. (2004). *Defect-Free Fatigue*. Lecture notes distributed in the unit 2.002 Mechanics and Materials II. Massachusetts Institute of Technology Department of Mechanical Engineering Cambridge, Spring, pp. 1–37. https://ocw.mit.edu/courses/2-002-mechanics-and-materials-ii-spring-2004/resources/lec21_notes/

[53] Dowling, N.E. (2004). Mean Stress Effects in Stress-Life and Strain-Life Fatigue. In *2nd SAE Brasil International Conference on Fatigue*. SAE Technical Paper 2004-01-2227. DOI: 10.4271/2004-01-2227.

[54] Wanhill, R.J.H. (2009). *Characteristic stress intensity factor correlations of fatigue crack growth in high strength alloys: reviews and completion of NLR investigations 1985-1990*. NLR-TP-2009-256. The Netherlands: National Aerospace Laboratory NLR.

[55] Musuva, J.K. and Radon, J.C. (2013). An elastic-plastic crack growth analysis using the J-integral concept.

[56] Tzamtzis, A. and Kermanidis, A.T. (2016). Fatigue crack growth prediction in 2xxx AA with friction stir weld HAZ properties. *Frattura ed Integrità Strutturale*, vol. 35, pp. 396–404. DOI: 10.3221/IGF-ESIS.35.45.

[57] Vikram, N. and Kumar, R. (2013). Review on fatigue-crack growth and finite element method. *International Journal of Scientific & Engineering Research*, vol. 4, no. 4, pp. 833–843.

[58] Chowdhury, P. and Sehitoglu, H. (2016). Mechanisms of fatigue crack growth – a critical digest of theoretical developments. *Fatigue & Fracture of Engineering Materials & Structures*, vol. 39, pp. 652–674, 2016. DOI: 10.1111/ffe.12392.

[59] Mann, T., Tveiten, B.W. and Härkegård, G. (2004). Fatigue of welded aluminium T-joints. In *ESIS-ECF 15 Sweden*, no. 1. From https://www.gruppofrattura.it/ocs/index.php/esis/ECF15/paper/viewFile/8703/4770

[60] Huang, X., Torgeir, M. and Cui, W. (2008). An engineering model of fatigue crack growth under variable amplitude loading. *International Journal of Fatigue*, vol. 30, no. 1, pp. 2–10. DOI: 10.1016/j.ijfatigue.2007.03.004.